Contents

A Framework **1**
A.1 Details of Datasets and Instructions 1
A.2 Details of Framework Application 5
A.3 Baselines Evaluation 5

B Method **6**
B.1 Discussion of Individual Encoding Module Method 6
B.2 Model Theoretical Capacity 7
B.3 Detalied Related Work 8

C Experiments **9**
C.1 Experiment setting 9
C.2 Detailed Zero-Shot Result 9
C.3 Detailed Few-Shot Results 11
C.4 Detailed Ablation Results of Pretraining 13
C.5 Instruction Robustness 13
C.6 Instruction Ablation 15
C.7 Attention Visualization 15

A Framework

A.1 Details of Datasets and Instructions

Table 1: Data Overview

Splitting	Data Class	Dataset	No. of Molecules	No. of Tasks	Task Metric	Task Type
Pretraining	Bioactivity assay	ChEMBL bioassay activity dataset	365065	1048	ROC_AUC	Classification
	Physico-chemical	CHEMBL Property	365065	13	RMSE	Regression
Downstream Zero-Shot	Large Scale	PCBA PubChem HTS bioAssay	437929	128	ROC-AUC	Classification
		ChEMBL Zero-Shot	91266	262	ROC_AUC	Classification
	Pharmacokinetic	CYP inhibition	16896	5	ROC_AUC	Classification
		BBBP Blood-brain barrier penetration	2039	1	ROC_AUC	Classification
	Bio-activity	MUV PubChem bioAssay	93087	17	ROC_AUC	Classification
		BACE-1 benchmark set	1513	1	ROC_AUC	Classification
		HIV replication inhibition	41127	1	ROC_AUC	Classification
	Toxicity	Tox21Toxicology in the 21st century	7831	12	ROC_AUC	Classification
		Toxcast	8598	617	ROC_AUC	Classification
	Physico-chemical	ESOL Water solubility	1128	1	RMSE	Regression
		FreeSolv Solvation free energy	642	1	RMSE	Regression
		Lipo Lipophilicity	4200	1	RMSE	Regression

The datasets used in our study are presented in Table 1. These datasets consist of different types of tasks related to molecule property prediction. It should be noted that during the pretraining phase, the loss function is not specific to the task types, but rather encompasses the generative loss of the language model.

We have chosen not to include certain datasets, namely SIDER and ClinTox, in our collection of datasets. The decision was based on the fact that the tasks associated with these datasets are not clearly defined and involve complex systemic phenomena, making it challenging to describe them through instructional texts. For instance, the ClinTox dataset involves determining whether drugs have passed the FDA approval, which is not an objective problem but rather a dynamic and intricate social phenomenon. The SIDER dataset focuses on describing the side effects of drugs on system organ classes, which have intricate mechanisms and a wide range of possible causes, making them difficult to be effectively conveyed through instructions.

For the Chembl property dataset that we have constructed, detailed information can be found in Table 2. These properties are sourced from the Chembl database [19] through the web API.

Table 2: Chembl property tasks and labels

Property	**Label type**
Aromatic rings number	Integer
cx_logd distribution coefficient	Real
cx_logp partition coefficient	Real
cx_most_apka $-\log_{10}$ dissociation constant	Real
Molecular masses	Real
Hydrogen bond donor number	Integer
Heavy atom number	Integer
Lipinski's rule of five violation number	Integer
Polar surface area (PSA)	Real
Quantitative Estimate of Druglikeness (QED)	Real
Rule of three passes	Bool
Rotatable bond number	Integer

The task explanation is primarily sourced from relevant papers, websites, or databases that introduce and compile the respective datasets. The specific sources utilized depend on the particular datasets under consideration. For Chembl tasks, we obtain task descriptions from the Chembl website. Descriptions for MoleculeNet tasks and PCBA are primarily sourced from the PubChem website. Certain datasets, such as Toxcast, include task descriptions within the dataset files. In the case of other tasks, like Chembl property and Physical-Chemical tasks, instructions are derived from Wiki or other papers. We list the instruction source in Table 3.

Table 3: Data sources and classes for different stages of the model

Dataset	Instruction Source
ChEMBL Zero-Shot bioassay activity dataset	Chembl Database
CHEMBL Property	Wiki
PCBA PubChem HTS bioAssay	Pubchem Database
ChEMBL Zero-Shot bioassay activity dataset	Chembl Database
CYP PubChem BioAssay CYP 1A2, 2C9, 2C19, 2D6, 3A4 inhibition	Pubchem Database
BBBP Blood-brain barrier penetration	Paper [21]
MUV PubChem bioAssay	Pubchem Database
BACE-1 benchmark set	Pubchem Database
HIV replication inhibition	Paper [38]
Tox21 Toxicology in the 21st century	Pubchem Database
Toxcast	Toxcast file
ESOL Water solubility	Paper [61]
FreeSolv Solvation free energy	Paper [7]
Lipo Lipophilicity	Wiki

The description covers a wide range of aspects, including the family, function, and mechanism of the assay target, the assay experiment setting, the approximation method used for determining the property, and others. We describe regression tasks by introducing the relasionship between the task property and other properties, i.e. how to estimate these properties by other ones. However, this method is still challenging due to the model's capacity to understand complex mathematical relationships.

The instructions for each task are generated automatically by conducting searches on the databases and summarizing the descriptions. We use a mixture strategy of summarizing, combining template-based summarizing and GPT-3.5-turbo-based summarizing methods. The GPT-3.5-turbo-based summarizing method is applied by the prompt 'Summarize the assay: \n {*Descriptions to be summarized*}'.

The resulting instructions are then concatenated with relevant questions. These instructions are subsequently reviewed and validated by a professional biology Ph.D. student and slightly modified if necessary.

We then list the instructions of each dataset. For datasets with more than one task, we only list the instruction of one task as an illustration.

Chembl

```
"The assay is PUBCHEM_BIOASSAY: qHTS Assay for Activators of
Human Muscle isoform 2 Pyruvate Kinase. (Class of assay:
confirmatory)  , and it is Direct single protein target
assigned . The assay has properties: assay category is
confirmatory ; assay organism is Homo sapiens ; assay type
description is Functional . Is the molecule effective to this
assay?"
```

Chembl property

```
  The   partition coefficient, abbreviated P, is defined as a
particular ratio of the concentrations of a solute between the
two solvents (a biphase of liquid phases), specifically for
un-ionized solutes, and the logarithm of the ratio is thus Log
P.  When one of the solvents is water and the other is a
non-polar solvent, then the log P value is a measure of
lipophilicity or hydrophobicity. The defined precedent is for
the lipophilic and hydrophilic phase types to always be in the
numerator and denominator respectively. What is the logarithm
of the partition coefficient of this molecule?
```

PCBA

```
"The assay tests the inhibition of ALDH1A1 activity using
propionaldehyde as an electron donor and NAD+ as an electron
acceptor. The conversion of NAD+ to NADH is measured via an
increase in fluorescence intensity to determine enzyme
activity. ALDH1A1 plays critical roles in the metabolic
activation of retinoic acid and may be a target for inhibitor
development in metabolic diseases. Is the molecule effective
to this assay?"
```

CYP450

```
"Find molecules that can effectively inhibit Cytochrome P450
(CYP450) enzymes, particularly CYP1A2, to help reduce the risk
of adverse drug events and drug-drug interactions caused by
CYP450-mediated metabolic pathways. Consider the various
CYP450 inhibition mechanisms such as occupying active sites or
weakening enzyme activity, while keeping in mind the potential
for increased side effects due to elevated blood drug
concentrations. Is this molecule effective to this assay?"
```

BBBP

```
"In general, molecules that passively diffuse across the brain
blood barrier have the molecular weight less than 500, with a
LogP of 2-4, and no more than five hydrogen bond donors or
acceptors. Does the molecule adhere to the three rules or not?"
```

MUV

```
"Protein kinase A (PKA) is an ubiquitous serine/threonine
protein kinase and belongs to the AGC kinase family. It has
several functions in the cell, including regulation of immune
response, transcription, cell cycle and apoptosis. PKA is a
cAMP dependent enzyme that exists in its native inactive form
```

```
as a 4 subunit enzyme with two regulatory and two catalytic
subunits. Binding of cAMP to the regulatory subunit leads to
the disassembly of the complex and release of now active
catalytic subunits. Is this molecule inhibitor of PKA?"
```

BACE

```
"BACE1 is an aspartic-acid protease important in the
pathogenesis of Alzheimer’s disease, and in the formation of
myelin sheaths. BACE1 is a member of family of aspartic
proteases. Same as other aspartic proteases, BACE1 is a
bilobal enzyme, each lobe contributing a catalytic Asp
residue, with an extended active site cleft localized between
the two lobes of the molecule. The assay tests whether the
molecule can bind to the BACE1 protein. Is this molecule
effective to the assay?"
```

HIV

```
"Human immunodeficiency viruses (HIV) are a type of
retrovirus, which induces acquired immune deficiency syndrome
(AIDs).  Now there are six main classes of antiretroviral
drugs for treating AIDs patients approved by FDA, which are
the nucleoside reverse transcriptase inhibitors (NRTIs), the
non-nucleoside reverse transcriptase inhibitors (NNRTIs), the
protease inhibitors, the integrase inhibitor, the fusion
inhibitor, and the chemokine receptor CCR5 antagonist.  Is
this molecule effective to this assay?"
```

Tox21

```
"Estrogen receptor alpha (ER aplha) is Nuclear hormone
receptor. The steroid hormones and their receptors are
involved in the regulation of eukaryotic gene expression and
affect cellular proliferation and differentiation in target
tissues. Ligand-dependent nuclear transactivation involves
either direct homodimer binding to a palindromic estrogen
response element (ERE) sequence or association with other
DNA-binding transcription factors, such as AP-1/c-Jun, c-Fos,
ATF-2, Sp1 and Sp3, to mediate ERE-independent signaling. Is
this molecule effective to this assay?"
```

Toxcast

```
"APR_HepG2_CellCycleArrest_24hr, is one of 10 assay
component(s) measured or calculated from the APR_HepG2_24hr
assay. It is designed to make measurements of cell phenotype,
a form of morphology reporter, as detected with fluorescence
intensity signals by HCS Fluorescent Imaging technology.Data
from the assay component APR_HepG2_CellCycleArrest_24hr was
analyzed into 2 assay endpoints. \nThis assay endpoint,
APR_HepG2_CellCycleArrest_24h_dn, was analyzed in the negative
fitting direction relative to DMSO as the negative control and
baseline of activity. \nUsing a type of morphology reporter,
measures of all nuclear dna for loss-of-signal activity can be
used to understand the signaling at the pathway-level as they
relate to the gene . \nFurthermore, this assay endpoint can be
referred to as a primary readout, because this assay has
produced multiple assay endpoints where this one serves a
signaling function. \nTo generalize the intended target to
other relatable targets, this assay endpoint is annotated to
```

```
the \"cell cycle\" intended target family, where the subfamily
is \"proliferation\". Is this molecule effective to this
assay?"
```

ESOL

```
"Solubility (logS) can be approximated by negative LogP -0.01
* (MPt \u2013 25) + 0.5 . Can you approximate the logS of this
molecule by its negative logP and MPt?"
```

FreeSolv

```
"The free energy of hydration can be approximated by
\u0394G_hyd = \u0394G_solv,soln - \u0394G_solv,gas + RT ln
(10^(-pKa)). Can you tell me the free energy of hydration (by
using the negative pka) of this molecule, predicted by using
\u0394G_solv and negative pka?"
```

Lipo

```
"Lipophilicity is an important feature of drug molecules that
affects both membrane permeability and solubility, measured by
octanol/water distribution coefficient (logD at pH 7.4).
What's the octanol/water distribution coefficient (logD at pH
7.4) of this molecule?"
```

A.2 Details of Framework Application

In our framework, we represent the labels of various tasks as strings. For assay tasks involving classification, the labels are converted to either "Yes" or "No" based on whether the molecule has an effect on the assay. In regression tasks, the labels are transformed into numerical strings. Integer values remain unchanged, while decimal numbers are rounded to two decimal places.

To conduct zero-shot testing on our model, we generate output sequences and extract the answer from the results. For assay classification, we consider the first token generated as the answer and use the scores for the 'Yes' and 'No' tokens to compute the ROC-AUC score for classification. In regression tasks, we extract the number from the generated sequence by performing string matching using a regular expression template: r"-?\d+\.?\d*e??\d*?". Notably, we discovered that GIMLET consistently generates results in the correct format for all classification tasks and accurately formatted numbers for over 98% of regression testing samples, without any augmentation of restriction in the vocabulary.

A.3 Baselines Evaluation

For the baselines, we apply our instruction-based molecule zero-shot learning to their respective settings. KVPLM employs SMILES for molecule representation and utilizes masked language modeling for molecule-text data. Galactica also represents molecules using SMILES but generates the next sentence in an autoregressive manner. MoMu employs contrastive learning between the GNN-encoded molecule and the corresponding text, allowing it to score each candidate sentence for the target molecule and retrieve the best matching one. Our application of each baseline model aligns with their intended use.

It is important to note that for the baseline models, to avoid baselines generating answers in classification not in our parsing method ('Yes' and 'No'), we limit the vocabulary during generation to only include 'Yes' and 'No' in classification tasks. This restriction is achieved by utilizing the bias term in huggingface to prevent the generation of other words. However, it is worth mentioning that our model, GIMLET, does *not* require this augmentation and is able to generate the desired outputs *without* any additional constraints.

For KVPLM, we mask the answer position in the whole sentence for the model to predict. For example, for molecule CCOc1ccccc1-n1nnnc1SCC(=O)NC(=O)NCc1ccco1 and classification tasks ARE inhibitor, input to KVPLM is:

```
"CCOc1ccccc1-n1nnnc1SCC(=O)NC(=O)NCc1ccco1
Oxidative stress has been implicated in the pathogenesis of a
variety of diseases ranging from cancer to neurodegeneration.
The antioxidant response element (ARE) signaling pathway is
important in the amelioration of oxidative stress. Is this
molecule agonists of antioxidant response element (ARE)
signaling pathway? [MASK]"
```

For Galactica, the answer is expected to be generated after reading the question. The input example is

```
"[START_I_SMILES] CCOc1ccccc1-n1nnnc1SCC(=O)NC(=O)NCc1ccco1
[END_I_SMILES]
Question: Oxidative stress has been implicated in the
pathogenesis of a variety of diseases ranging from cancer to
neurodegeneration. The antioxidant response element (ARE)
signaling pathway is important in the amelioration of
oxidative stress. Is this molecule agonists of antioxidant
response element (ARE) signaling pathway?
Answer:"
```

For MoMu, we compute the matching score between the molecule graph and the instruction with each answer. In the example, the classification scores for 'Yes' and 'No' are computed by matching graph feature of molecule CCOc1ccccc1-n1nnnc1SCC(=O)NC(=O)NCc1ccco1 with

```
"Oxidative stress has been implicated in the pathogenesis of a
variety of diseases ranging from cancer to neurodegeneration.
The antioxidant response element (ARE) signaling pathway is
important in the amelioration of oxidative stress. Is this
molecule agonists of antioxidant response element (ARE)
signaling pathway? Yes"
```

and

```
"Oxidative stress has been implicated in the pathogenesis of a
variety of diseases ranging from cancer to neurodegeneration.
The antioxidant response element (ARE) signaling pathway is
important in the amelioration of oxidative stress. Is this
molecule agonists of antioxidant response element (ARE)
signaling pathway? No"
```

.

B Method

B.1 Discussion of Individual Encoding Module Method

The Individual encoding module-based multimodal language model can be formalized as $\mathrm{LLM}(M(G), T)$, where M is the individual encoding module for graph data G. For example, the visual module is applied to pre-encode the image data to get the dense representation, then put into the language model as tokens embedding [4, 9, 1, 28]. Current works on molecule language models also use a GNN to get the representation of molecules to interact with the language models [16, 49, 48].

This method can be considered as decomposition of the conditional probability $P(y|G, T)$

$$P(\hat{y}|G,T) = \int P_M(z|G) P_{\mathrm{LLM}}(\hat{y}|z,T) dz, \tag{1}$$

based on the assumption that the feature distributions $P(z|G)$ should be modeled by modality-specific modules to introduce inductive bias, and be independent of text information to help with adaptation to novel text data.

However, for the molecule-text model, individual pre-encoding modules present problems. First, graph learning relies on structure information, but the dense vectors encoded by GNN have a limited capacity to carry structure information, and language models don't have inductive bias toward graph structure. Furthermore, training the additional module is difficult due to the increased layers, since deep transformers have vanishing gradients in early layers [29, 2], which is a well-known problem of transformer. Lastly, the additional modules increase parameters and training costs.

Our method GIMLET not only overcome these issues, our approach GIMLET not only directly unifies the standard language model for graph and text *without* introducing additional graph encoder module, but also remains the decoupled graph encoding for better generalization.

B.2 Model Theoretical Capacity

In this section, we analyze the theoretical capacity of our modeling method.

Theorem 1 *Assume for different input features and position embeddings, the transformer layers can output different output features. The transformer with distance-based relative position embedding has a stronger capacity than the 1-WL test for the graph isomorphism problem.*

Proof 1 *The 1-WL test is defined as the following iteration:*

$$\begin{aligned} &\chi_G^0(i) = \mathrm{hash}(v_i) \\ &\chi_G^t(i) := \mathrm{hash}\left(\chi_G^{t-1}(i), \{\chi_G^{t-1}(j) : j \in \mathcal{N}_G(i)\}\right) (\forall i \in N), \end{aligned} \tag{2}$$

where χ_G is the label in WL test, hash *is the hash function, $\mathcal{N}_G(i)$ is the neighbor of node i.*

The transformer with distance-based relative position embedding can be considered as the following mapping:

$$\begin{aligned} \chi_G^t(i) &:= \mathrm{hash}\left(\left\{\left(d_G(i,j), \chi_G^{t-1}(j)\right) : j \in N\right\}\right) \\ &= \mathrm{hash}(\{(0, \chi_G^{t-1}(i))\} \\ &\cup \{(1, \chi_G^{t-1}(j)) : j \in \mathcal{N}_G(i)\} \\ &\cup \{(d_G(i,k), \chi_G^{t-1}(k)) : k \in N - \mathcal{N}_G(i) - \{i\}\}) \end{aligned} \tag{3}$$

It can be seen that the iteration of the transformer with distance-based relative position embedding includes both the node i and its neighbors $\mathcal{N}_G(i)$, marked by distance 0 and 1, respectively, ensuring the capacity is at least as strong as 1-WL test. It further includes other nodes far away, along with their distance, which constitutes a stronger capacity than 1-WL test. Figure 1 are two example graphs that cannot be distinguished by 1-WL test, but can be distinguished by transformer with distance-based relative position embedding.

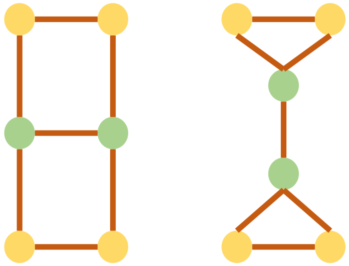

Figure 1: Two example graphs that cannot be distinguished by 1-WL test, but can be distinguished by transformer with distance-based relative position embedding.

Theorem 2 *Assume for different input features and position embeddings, the transformer layers can output different output features.* GIMLET *can distinguish graph-instruction pairs if graphs can be* *distinguished by transformer with distance-based relative position embedding, or instructions are different.*

Proof 2 *As* GIMLET *decomposes the attention from graph nodes to text, the graph nodes can only attend to other graph nodes. Thus the encoding capacity of graph data is the same as a single transformer with distance-based relative position embedding for graph data.*

Along with the assumption of transformer layers, GIMLET *is able to distinguish graph-instruction pairs if graphs can be distinguished by transformer with distance-based relative position embedding, or instructions are different.*

B.3 Detalied Related Work

We present a detailed related work here, due to the space limitation of paper.

Molecule Representation learning In recent years, there has been a growing interest in developing molecular representation learning for downstream tasks like drug discovery and other applications. One approach that has received considerable attention is utilizing language modeling techniques to acquire molecular representations based on Simplified Molecular Input Line Entry System (SMILES) strings [57, 10]. Although sequence-based representations have demonstrated success in some applications, concerns have been raised about their capability to incorporate all pertinent substructure information. To address this limitation, some researchers have proposed the use of Graph Neural Networks (GNNs) to model molecules as graphs [20, 67, 25], potentially providing a more comprehensive and accurate representation of the molecular structure.

Existing GNNs follow the message-passing paradigm and suffer from problems like long-range dependency vanishing and over-smoothing. Recently, Graph Transformer [44, 65] has been proposed to better encode structures of graphs. The Graph Transformer is inspired by the Transformer architecture, which has shown remarkable performance in natural language processing [55, 13, 33]. The Graph Transformer extends the Transformer architecture to the graph domain, allowing the model to capture the global structure and long-range dependencies of the graph [69, 14, 27, 26, 62, 40, 34, 65, 8, 35, 11, 5, 22, 71].

Molecule Pretraining To fully explore the inherent structural information of molecules on a large scale and transfer useful information to downstream tasks, significant efforts have been made to address the inadequacies in molecular pre-training. Supervised pretraining is commonly used for learning useful representations [25, 65, 52]. As for unsupervised pretraining, one approach involved using an generative pre-training strategy on molecular SMILES strings [57, 24, 10, 3, 45] and Graph [25, 30, 44, 70], which was followed by recent works adopting the contrastive paradigm that aligns representation of augmented views of the same graph but keeping views from other graphs away [56, 50, 23, 67, 66, 53, 64, 18, 51, 59, 63, 58, 32].

The pretraining methods mentioned focus on obtaining representations for supervised training. However, for natural language instruction-based zero-shot graph learning, it's necessary to incorporate natural language into the pretraining process. Several studies have explored molecule structure-text multimodal pretraining. One class of method is the SMILES based language model, including KVPLM [68] and MolT5 [15], which use SMILES strings and text for joint representation and translation. Another work Galactica [54] explored the multi-task molecule task learning with instruction. Some other works acquire advanced representations for molecules by GNN, such as Text2Mol [16], MoMu [49], MoleculeSTM [31], and CLAMP [48], trained by contrastive learning between molecule graph and text description for molecule retrieval and caption tasks. MoleculeSTM and CLAMP explored molecule editing and property prediction with instructions. However, none of these works address the zero-shot fashion on complex molecule tasks like property prediction, due to constraints imposed by the pretraining methodology that not addressing the instruction-following ability, and their model capacity for representing molecule graphs.

Instruction-based zero-shot learning Instruction-based zero-shot learning is an innovative approach that leverages natural language instructions and definitions to enable neural models to solve a variety of tasks [42, 6, 47, 17, 72, 36, 37, 41]. By providing a human-readable prompt, this method enables easier and more efficient specification of the learning task by utilizing knowledge about the task without data. To enhance the model's ability to follow instructions, some researchers have employed instruction-based pretraining techniques [46, 60, 12, 39], which explicitly train language models to solve tasks with instructions. Besides natural language processing, instruction-based zero-shot learning is also studied in multimodal domains like images [4, 9, 1, 28].

C Experiments

C.1 Experiment setting

Our model only utilizes the basic features [25, 52] of molecule graphs, which do not include additional features like ring markers. Specifically, it utilizes the first two dimensions of node features and the first two dimensions of edge features processed by ogb.smiles2graph. Therefore, the effectiveness of GIMLET predominantly stems from its architectural design and pretraining rather than the graph features it incorporates.

Following the standard supervised setting in previous studies [25], we utilize the scaffold strategy [43] to partition datasets into three subsets: the training set, validation set, and testing set with a ratio of 0.8, 0.1, 0.1. The scaffold strategy is a deterministic approach that involves sorting the data based on the scaffold, which represents the molecular structure. While this strategy aids in dataset partitioning, it can introduce a significant domain gap between the training and testing sets, thereby increasing the challenge of generalization.

For zero-shot, we report the results on the testing sets, ensuring the comparability of our results to previous works. For few-shot, we report the result of the best validation model on the testing set, the same as previous works and other supervised baselines [43].

Many datasets encompass multiple tasks. To evaluate these datasets, we conduct separate testing for each task, accompanied by their respective instructions. For datasets with multiple tasks, we report the average ROC-AUC score for each task, following the methodology established in previous works [25].

C.2 Detailed Zero-Shot Result

We list the full zero-shot result of GIMLET and baselines in Table 4, 5, and 6. The standard deviation for supervised results are denoted after ±, and the multi-task setting results of Galactica are denoted in parentheses with italic. We also include the instruction-based zero-shot result reported in recent baseline CLAMP [48] which is tested by their instruction, denoted by italics too. CLAMP is a contrastive pretrained model with ensembled encoders for molecule and text. The parameter number for CLAMP's result is not clearly stated in their paper but should be larger than 10B as they use sT5 language model [42] XXL variant (11B) as one of the ensembled language models.

Table 4: Zero shot performance over Bio-activity tasks

Method	Parameter	Type	bace	hiv	muv	Avg. bio
KVPLM	110M	Zero Shot	0.5126	0.6120	0.6172	0.5806
MoMu	113M		0.6656	0.5026	0.6051	0.5911
CLAMP	> 10B		*0.6476*	*0.8067*	-	-
GIMLET	64M		0.6957	0.6624	0.6439	0.6673
Galactica-125M	125M	Multi Task	0.4451(*0.561*)	0.3671(*0.702*)	0.4986	0.4369
Galactica-1.3B	1.3B		0.5648(*0.576*)	0.3385(*0.724*)	0.5715	0.4916
GCN	0.5M	Supervised	*0.736±0.030*	*0.757±0.011*	*0.732±0.014*	0.742
GAT	1.0M		*0.697±0.064*	*0.729±0.018*	*0.666±0.022*	0.697
GIN	1.8M		*0.701±0.054*	*0.753±0.019*	*0.718±0.025*	0.724
Graphormer	48M		0.7760±0.015	0.7452±0.014	0.7061±0.027	0.7424
Graphormer-p	48M		0.8575±0.006	0.7788±0.012	0.7480±0.020	0.7948

The result in parentheses represents the outcome of the multitask setting, also referred to as weakly supervised in the original paper, where the same instructions are used for both pretraining and testing. While Galactica has been exposed to the same task instructions, it actually employs multitask learning with instructions serving as task identity.

Even in comparison to Galactica's multitask result, GIMLET demonstrates comparable or superior performance on most datasets. This highlights the ability of GIMLET to perform zero-shot tasks with high quality.

Table 5: Zero shot performance over Toxicity tasks

Method	Parameter	Type	tox21	toxcast	Avg. tox
KVPLM	110M	Zero Shot	0.4917	0.5096	0.5007
MoMu	113M		0.5757	0.5238	0.5498
CLAMP	> 10B		*0.6058*	*0.5383*	0.5721
GIMLET	64M		0.6119	0.5904	0.6011
Galactica-125M	125M	Multi Task	0.4964(*0.543*)	0.5106(*0.518*)	0.5035
Galactica-1.3B	1.3B		0.4946(*0.606*)	0.5123(*0.589*)	0.5035
GCN	0.5M	Supervised	*0.749±0.008*	*0.633±0.009*	0.691
GAT	1.0M		*0.754±0.005*	*0.646±0.006*	0.700
GIN	1.8M		*0.740±0.008*	*0.634±0.006*	0.687
Graphormer	48M		0.7589±0.004	0.6470±0.008	0.7029
Graphormer-p	48M		0.7729±0.006	0.6649±0.006	0.7189

Table 6: Zero shot performance over Pharmacokinetic tasks

Method	Parameter	Type	bbbp	cyp450	Avg. pha
KVPLM	110M	Zero Shot	0.6020	0.5922	0.5971
MoMu	113M		0.4981	0.5798	0.5390
CLAMP	> 10B		*0.4788*	-	-
GIMLET	64M		0.5939	0.7125	0.6532
Galactica-125M	125M	Multi Task	0.6052(*0.393*)	0.5369	0.5711
Galactica-1.3B	1.3B		0.5394(*0.604*)	0.4686	0.5040
GCN	0.5M	Supervised	*0.649±0.030*	*0.8041±0.005*	0.7266
GAT	1.0M		*0.662±0.026*	0.8281±0.004	0.7451
GIN	1.8M		*0.658±0.045*	0.8205±0.012	0.7392
Graphormer	48M		0.7015±0.013	0.8436±0.003	0.7725
Graphormer-p	48M		0.7163±0.009	0.8877±0.004	0.8020

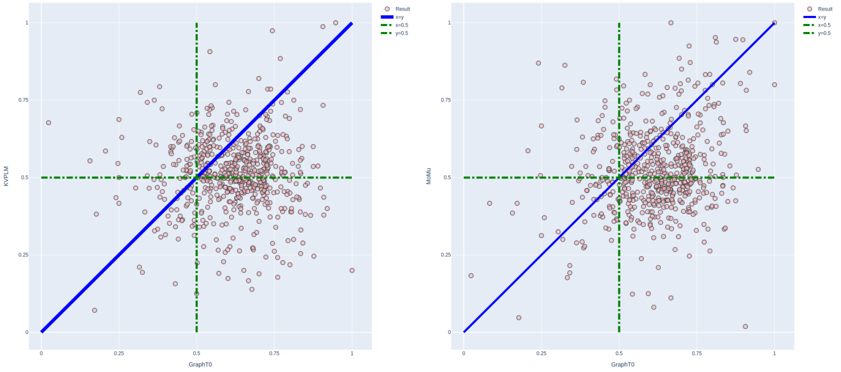

Figure 2: Scatter of GIMLET over baselines. Below the diagonal line x=y means our method performs better.

The disparity between the multitask result and the tested result with our instructions is due to the gap between their instructions and ours, which indicates that Galactica relies on specific task instructions for task recognition, without a true understanding of the instructions. As a result, it exhibits poor generalization to other instruction forms. Note that Galactica even do not surpass KVPLM and MoMu which are also zero-shot learning methods.

GIMLET exhibits superior performance compared to the larger model CLAMP on the majority of datasets, with the exception of HIV. It is important to highlight that our model is significantly smaller in size than CLAMP, underscoring the effectiveness of our unified graph-text language model. Additionally, it should be noted that CLAMP lacks the capability to handle regression tasks due to its contrastive model architecture, whereas our encoder-decoder architecture enables us to successfully tackle a wide range of task types.

Significantly, the supervised results shed light on the task difficulties associated with each dataset. This showcases GIMLET's capability to effectively solve molecule tasks in a zero-shot manner, approaching the performance of supervised results. Furthermore, our pretraining tasks yield an average performance improvement of 3 percent for Graphormer, with the largest gains observed in Bioactivity tasks and the smallest in Toxicity tasks. This suggests that there still exist gaps between the pretraining data and our downstream tasks, addressing the zero-shot setting of our dataset.

In Figure 2, we present scatter plots comparing GIMLET with KVPLM and MoMu across all tasks. The diagonal line represents the equality line where x=y indicates our method outperforms the baseline. Notably, it is evident that GIMLET consistently performs significantly better than random guessing and surpasses the baselines on all tasks.

We plot the scatter of regression tasks in Figure 3. The plot clearly demonstrates a strong correlation between the predicted and actual values for ESOL and Lipo.

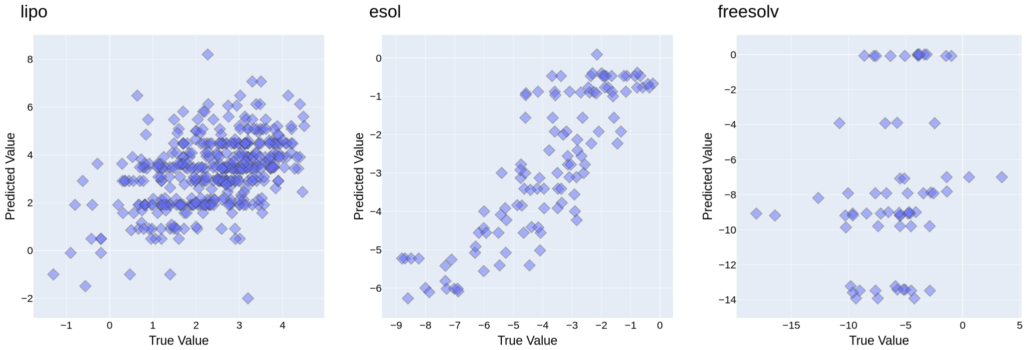

Figure 3: Scatter of GIMLET on generative tasks.

C.3 Detailed Few-Shot Results

In both classification tasks and regression tasks, we fine-tune the last linear layer of all models using their respective modeling loss.

It is important to note that the instruction-based few-shot approach is trained on each task individually, while supervised baselines are trained on multiple tasks from the dataset. Therefore, comparing these two approaches may not be strictly fair, as the multitask learning of the supervised baseline can contribute to improved task performance.

The results for few-shot learning on each dataset are presented in Figure 4. It is evident that, across the majority of datasets, GIMLET demonstrates improvement as the number of few-shot examples increases. In fact, it even outperforms or matches the performance of the supervised GIN on several datasets, such as bace, bbbp, and esol. There is also observable enhancement in performance across various datasets when employing few-shot learning, including tox21, toxcast, lipo, and freesolv.

There is not result of MoMu on regression tasks, because MoMu is a contrastive model between graph and text, which cannot handle regression tasks.

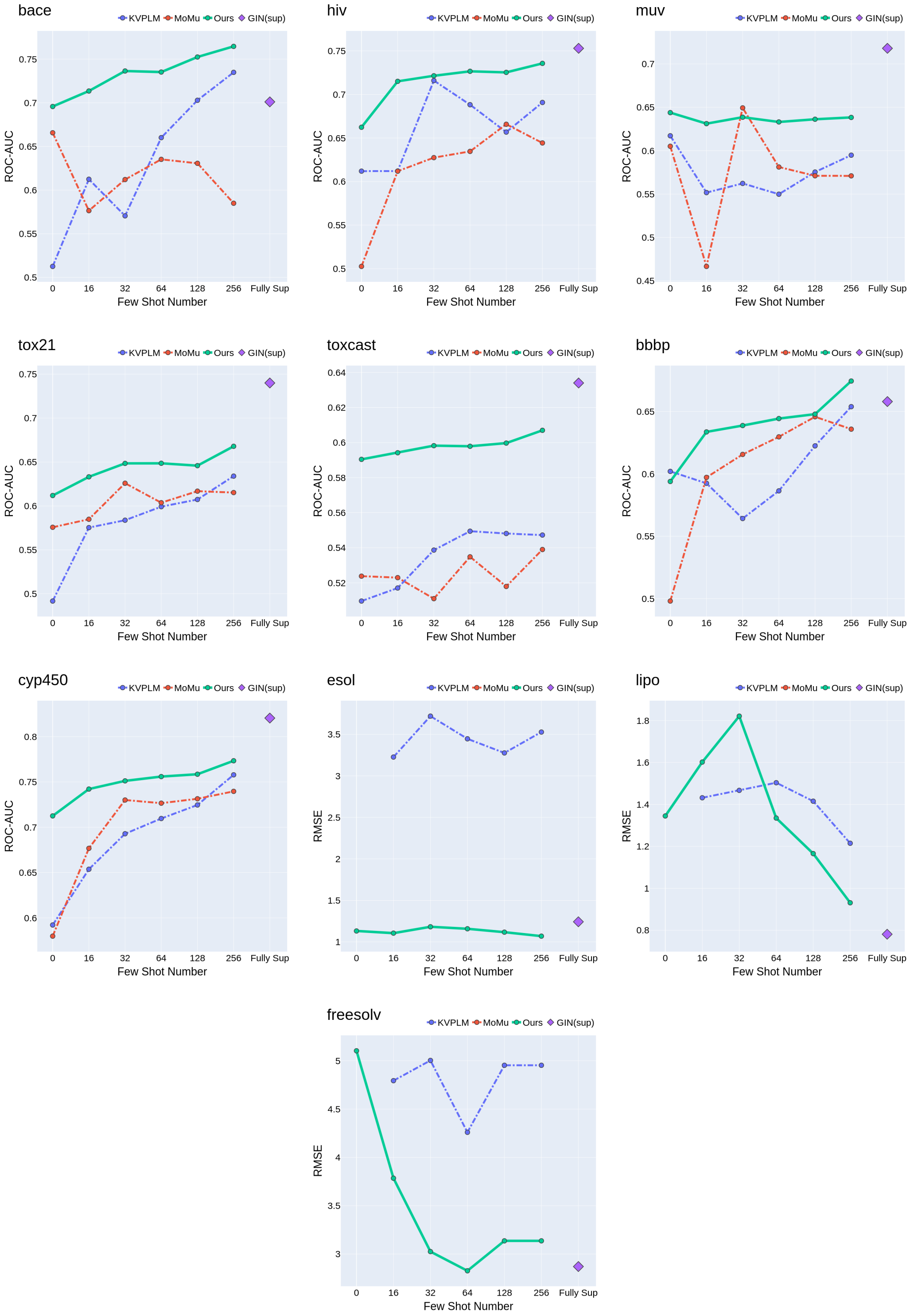

Figure 4: Few-shot performance on each dataset

C.4 Detailed Ablation Results of Pretraining

The results of pretraining ablation for each dataset are presented in Table 7, 8, 9, and 10. The findings indicate that both bioactivity assay and physico-chemical properties offer significant benefits for all the downstream tasks, demonstrating positive transfer across different domains.

Table 7: Pretraining ablation study on Bio-activity tasks

	bace	hiv	muv	Average_bio
bioactivity assay only	0.6390	0.6772	0.6044	0.6402
physico-chemical only	0.4648	0.5461	0.4572	0.4894
both	0.6957	0.6624	0.6439	0.6673

Table 8: Pretraining ablation study on Toxicity tasks

	tox21	toxcast	Average_tox
bioactivity assay only	0.5726	0.5625	0.5676
physico-chemical only	0.4478	0.5017	0.4748
both	0.6119	0.5904	0.6011

Table 9: Pretraining ablation study on Pharmacokinetic tasks

	bbbp	cyp450	Average_pha
bioactivity assay only	0.5313	0.6829	0.6071
physico-chemical only	0.5932	0.4976	0.5454
both	0.5939	0.7125	0.6532

C.5 Instruction Robustness

To test the robustness of GIMLET, the Instructions are rephrased by GPT-3.5-turbo. There are four types of rephrasing, realized by the following prompts:

rewrite

```
'Rephrase the text of the following prompt: \n'
```

expand

```
'Rephrase the text of the following prompt longer: \n'
```

detail

```
'Rephrase the text of the following prompt by adding more
explanation: \n'
```

short

```
'Rephrase the text of the following prompt shorter: \n'
```

Given a task instruction, we rephrase the instruction by the prompts above. Here is an example of four types of rephrased task instruction from Toxcast:

origin

```
"CEETOX_H295R_ANDR, is one of 23 assay component(s) measured
or calculated from the CEETOX_H295R assay. It is designed to
make measurements of hormone induction, a form of inducible
reporter, as detected with absorbance signals by HPLC-MS-MS
technology.Data from the assay component CEETOX_H295R_ANDR was
analyzed into 2 assay endpoints. This assay endpoint,
CEETOX_H295R_ANDR_dn, was analyzed in the positive fitting
direction relative to DMSO as the negative control and
baseline of activity. Using a type of inducible reporter,
```

Table 10: Pretraining ablation study on Physical-chemical tasks

	esol	freesolv	lipo	Average_phy
bioactivity assay only	-	-	-	
physico-chemical only	1.1822	5.2935	1.3778	2.6178
both	1.1320	5.1027	1.3450	2.5266

```
loss-of-signal activity using HPLC-MS-MS was used to
understand synthesis of Androstenedione in H295R cell line at
48hr of chemical exposure. To generalize the intended target
to other relatable targets, this assay endpoint is annotated
to the steroid hormone intended target family, where the
subfamily is androgens. Is this molecule effective to this
assay?"
```

rewrite

```
"The CEETOX_H295R_ANDR is a component of the CEETOX_H295R
assay, which measures hormone induction through absorbance
signals detected by HPLC-MS-MS technology. The data from
CEETOX_H295R_ANDR has been analyzed into two endpoints, with
CEETOX_H295R_ANDR_dn being analyzed in relation to DMSO as the
negative control and baseline of activity. HPLC-MS-MS was used
to detect loss-of-signal activity and understand the synthesis
of Androstenedione in H295R cell line after 48 hours of
chemical exposure. This assay endpoint is related to the
steroid hormone intended target family, specifically the
subfamily of androgens, and can be generalized to other
similar targets.Can this assay be effectively performed using
this molecule?"
```

expand

```
"The CEETOX_H295R_ANDR assay component is just one of the 23
assay components that are measured or calculated from the
CEETOX_H295R assay. The assay is specifically designed to
measure hormone induction, which is a form of inducible
reporter, and is detected using absorbance signals by means of
HPLC-MS-MS technology. The data obtained from the
CEETOX_H295R_ANDR assay component was analyzed into two assay
endpoints. The CEETOX_H295R_ANDR_dn assay endpoint was
analyzed in the positive fitting direction in relation to DMSO
as the negative control and activity baseline. To understand
the synthesis of Androstenedione in the H295R cell line after
48 hours of chemical exposure, loss-of-signal activity was
used with HPLC-MS-MS technology. This endpoint is annotated to
the steroid hormone intended target family to help other
related targets, where the subfamily is androgens. Can it be
determined if this particular molecule exhibits desirable
efficacy to be utilized in this particular assay?"
```

detail

```
"The CEETOX_H295R_ANDR is an assay component that is one of
the 23 components that are measured or calculated from the
CEETOX_H295R assay. It is intended to measure hormone
induction, which is a form of inducible reporter, and the
measurement is done with the help of absorbance signals using
HPLC-MS-MS technology. The data obtained from the measurement
of assay component CEETOX_H295R_ANDR is analyzed into two
assay endpoints. One of these endpoints, CEETOX_H295R_ANDR_dn,
is analyzed in the positive fitting direction, relative to
DMSO, which is used as the negative control and baseline for
activity. The HPLC-MS-MS technology is used to detect the
loss-of-signal activity, which helps in understanding the
synthesis of Androstenedione in H295R cell line after 48 hours
of chemical exposure. To make the intended target more
comprehensive and relatable to other targets, the assay
endpoint is annotated to the steroid hormone intended target
family, where the subfamily is androgens. Can this molecule be
used for this assay?"
```

short

```
"CEETOX_H295R_ANDR is one of 23 components in the CEETOX_H295R
assay, measuring hormone induction detected with absorbance
signals by HPLC-MS-MS. It's analyzed into 2 endpoints, with
CEETOX_H295R_ANDR_dn being the positive fitting direction
relative to the negative control. It analyzes the
loss-of-signal activity to understand Androstenedione
synthesis in H295R cell line after 48hr chemical exposure.
It's annotated as a steroid hormone intended target in
androgens sub-family. Is molecule suitable for assay?"
```

C.6 Instruction Ablation

To ablate the explanation-based instruction, we remove the explanation and only keep the assay name. The ablated instruction for the instruction above is:

```
"The assay name is CEETOX_H295R_ANDR. Is this molecule
effective to this assay?"
```

C.7 Attention Visualization

We present visualizations of the attention of text tokens to molecule graphs, demonstrating how our unified transformer incorporates molecule information using various instructions. We randomly sample molecules and attention heads for visualization. To emphasize high-level features, we focus on visualizing the attention patterns of the last layer. The redder means the larger attention value.

For BACE instruction, we visualize the attention of several keywords marked in red to molecules:

"BACE1 is an aspartic-acid protease important in the pathogenesis of Alzheimer's disease, and in the formation of myelin sheaths. BACE1 is a member of family of aspartic proteases. Same as other aspartic proteases, BACE1 is a bilobal enzyme, each lobe contributing a catalytic Asp residue, with an extended active site cleft localized between the two lobes of the molecule. The assay tests whether the molecule can bind to the BACE1 protein. Is this molecule effective to the assay?"

For BBBP instruction:

'In general, molecules that passively diffuse across the brain blood barrier have the molecular weight less than 500, with a LogP of 2-4, and no more than five hydrogen bond donors or acceptors. Does the molecule adhere to the three rules or not?'

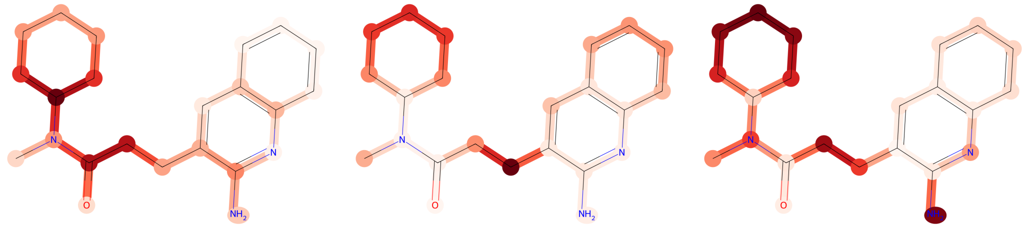

(a) BACE1 (b) aspartic-acid (c) Alzheimer

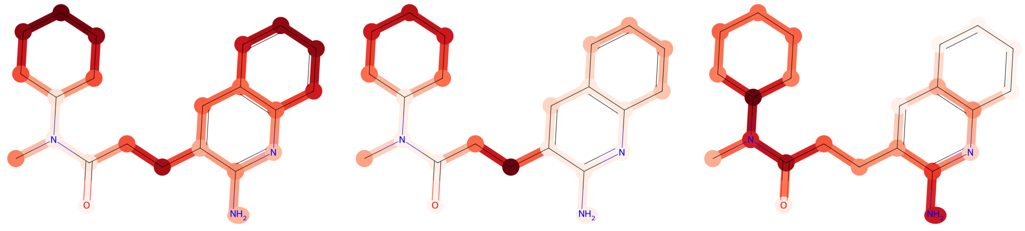

(d) myelin (e) aspartic (f) bilobal

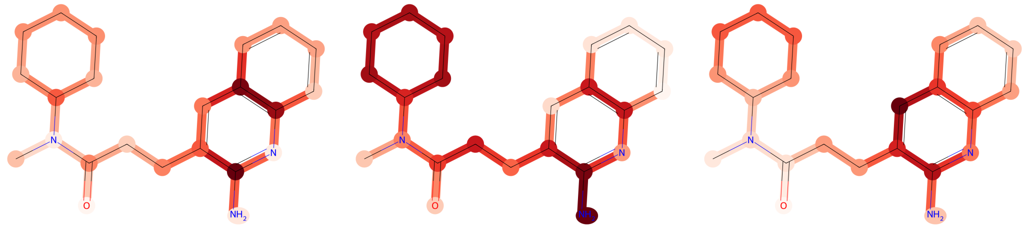

(g) catalytic (h) cleft (i) effective

Figure 5: Visualization of attention for BACE on molecule
O=C(N(C)C1CCCCC1)CCc1cc2c(nc1N)cccc2

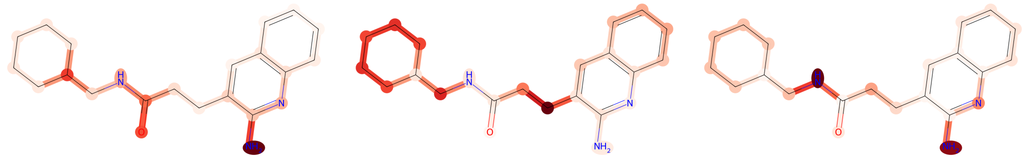

(a) BACE1 (b) aspartic-acid (c) Alzheimer

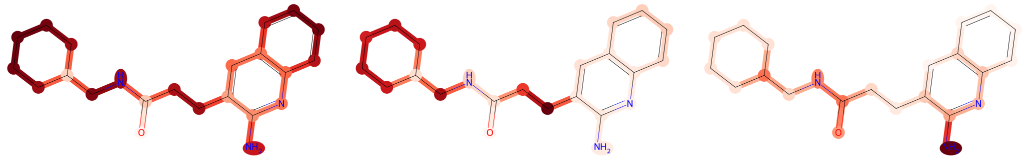

(d) myelin (e) aspartic (f) bilobal

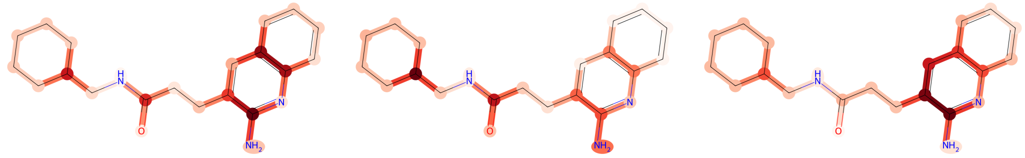

(g) catalytic (h) cleft (i) effective

Figure 6: Visualization of attention for BACE on molecule O=C(NCC1CCCCC1)CCc1cc2c(nc1N)cccc2

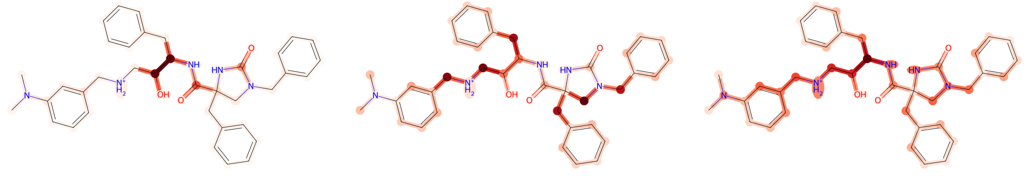

(a) BACE1 (b) aspartic-acid (c) Alzheimer

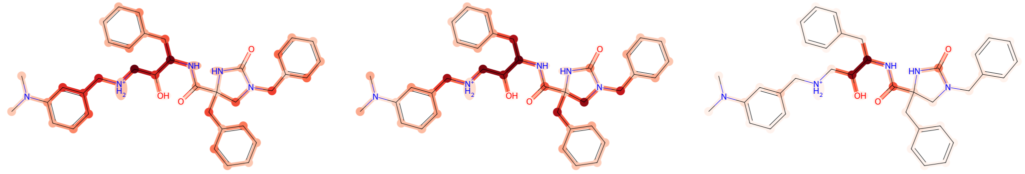

(d) myelin (e) aspartic (f) bilobal

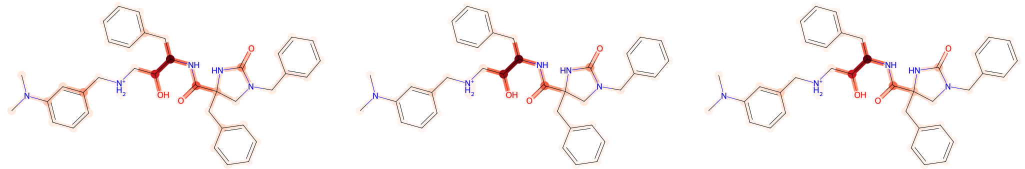

(g) catalytic (h) cleft (i) effective

Figure 7: Visualization of attention for BACE on molecule O=C1NC(CN1Cc1ccccc1)(Cc1ccccc1)C(=O)NC(Cc1ccccc1)C(O)C[NH2+]Cc1cc(N(C)C)ccc1

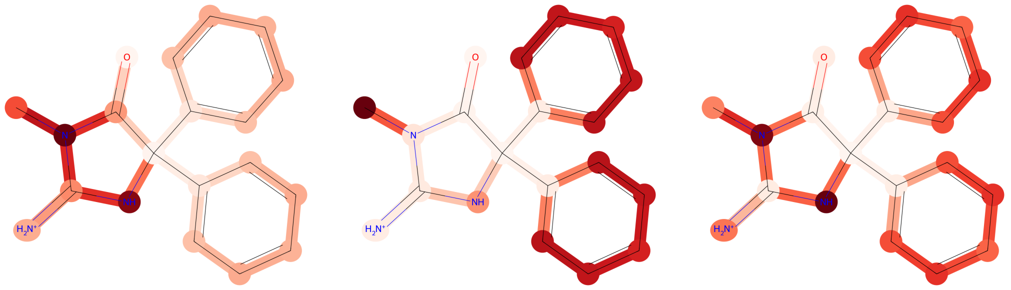

(a) BACE1 (b) aspartic-acid (c) Alzheimer

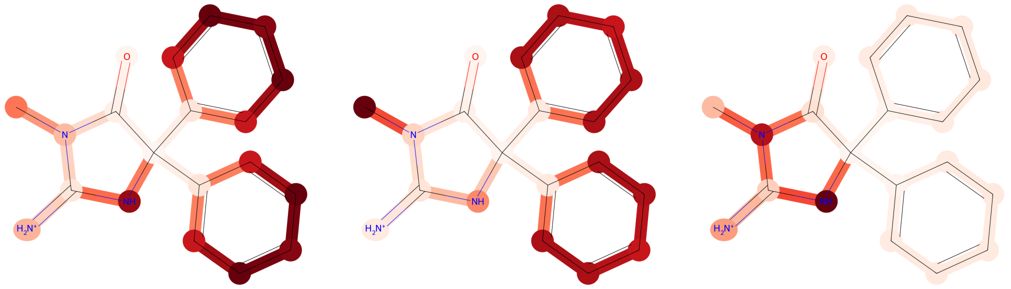

(d) myelin (e) aspartic (f) bilobal

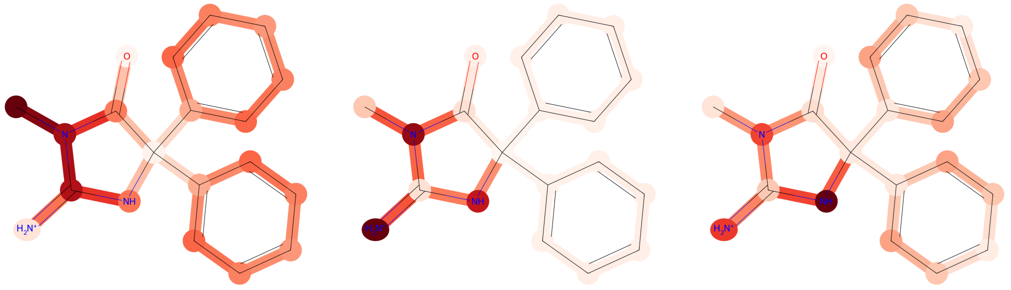

(g) catalytic (h) cleft (i) effective

Figure 8: Visualization of attention for BACE on molecule O=C1N(C)C(=[NH2+])NC1(c1ccccc1)c1ccccc1

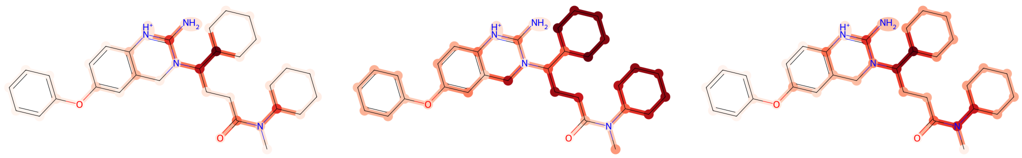

(a) BACE1 (b) aspartic-acid (c) Alzheimer

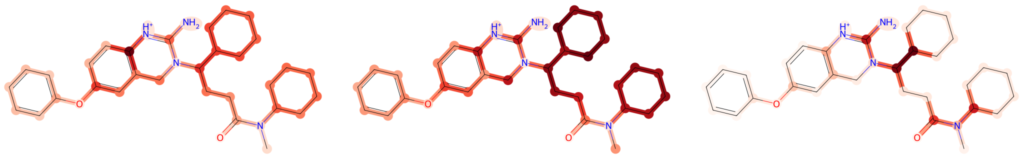

(d) myelin (e) aspartic (f) bilobal

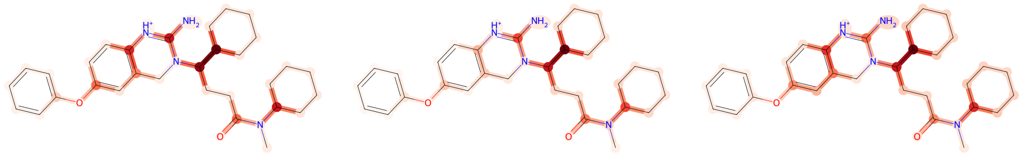

(g) catalytic (h) cleft (i) effective

Figure 9: Visualization of attention for BACE on molecule
O(c1cc2CN(C(CCC(=O)N(C)C3CCCCC3)C3CCCCC3)C(=[NH+]c2cc1)N)c1ccccc1

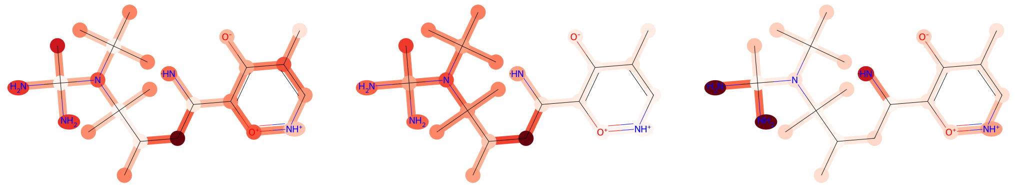

(a) brain blood barrier (b) molecular weight (c) 500

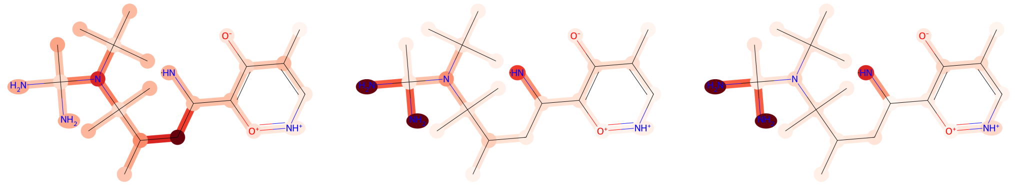

(d) LogP (e) 2-4 (f) five

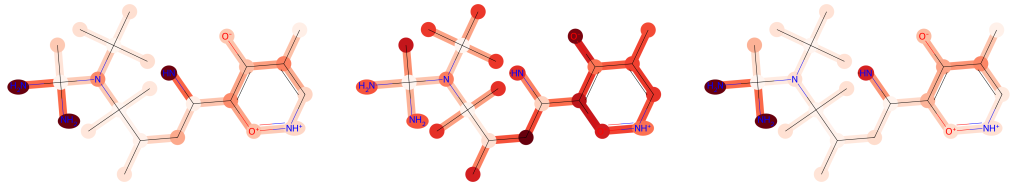

(g) hydrogen bond donors (h) acceptors (i) three rules

Figure 10: Visualization of attention for BBBP on molecule
NH
C(CC(C)C([N@@](C(C)(C)C)C(N)(C)N)(C)C)c1c(c(c[nH+][o+]1)C)[O-]

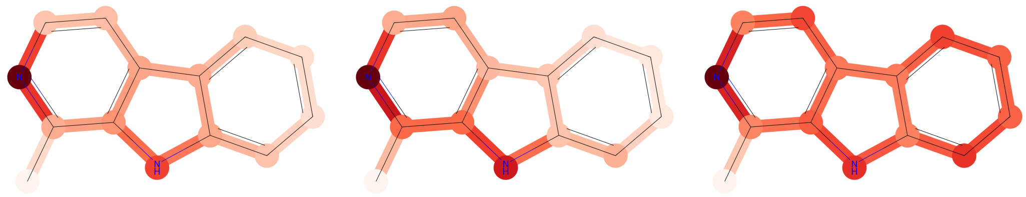

(a) brain blood barrier (b) molecular weight (c) 500

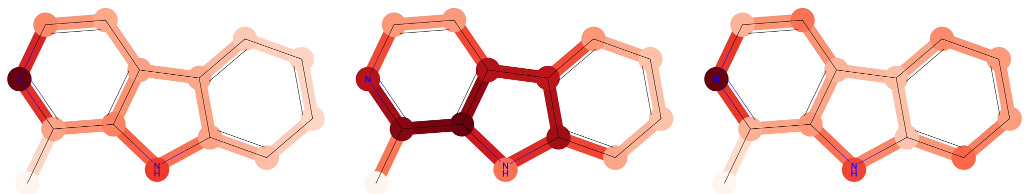

(d) LogP (e) 2-4 (f) five

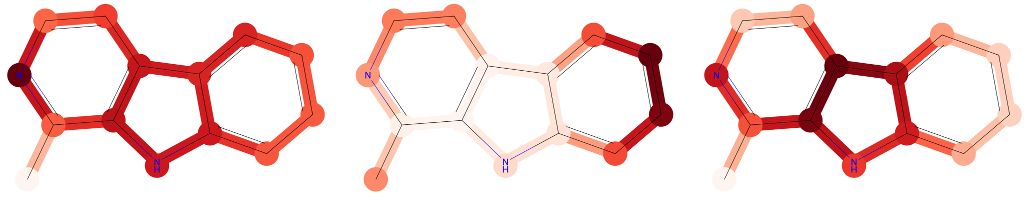

(g) hydrogen bond donors (h) acceptors (i) three rules

Figure 11: Visualization of attention for BBBP on molecule Cc1nccc2c1[nH]c3ccccc23

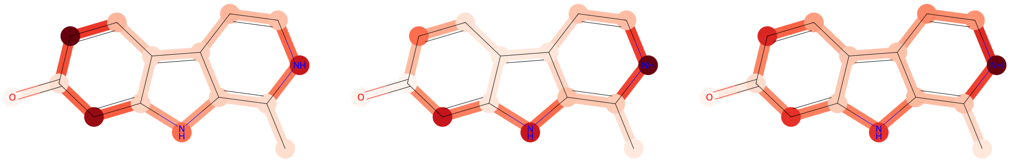

(a) brain blood barrier (b) molecular weight (c) 500

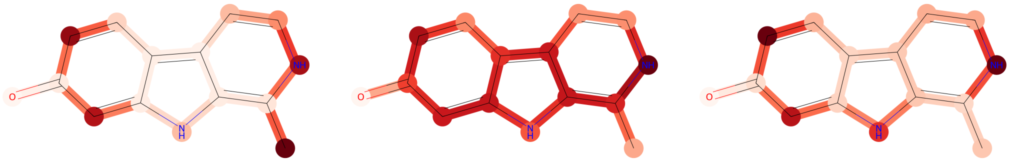

(d) LogP (e) 2-4 (f) five

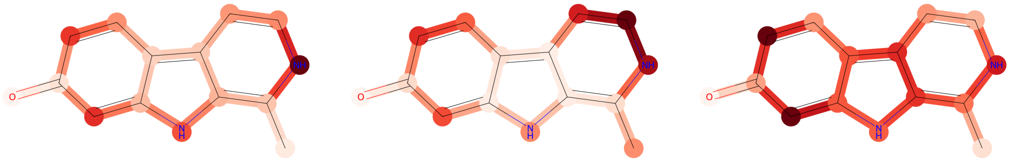

(g) hydrogen bond donors (h) acceptors (i) three rules

Figure 12: Visualization of attention for BBBP on molecule CC1=C2NC3=CC(=O)C=CC3=C2C=CN1

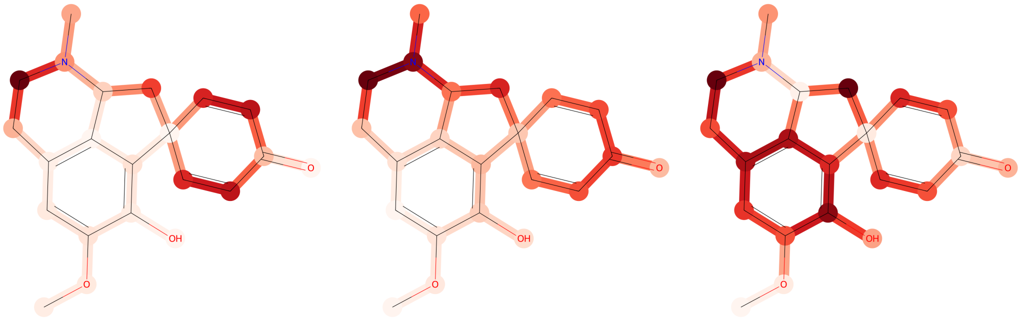

(a) brain blood barrier (b) molecular weight (c) 500

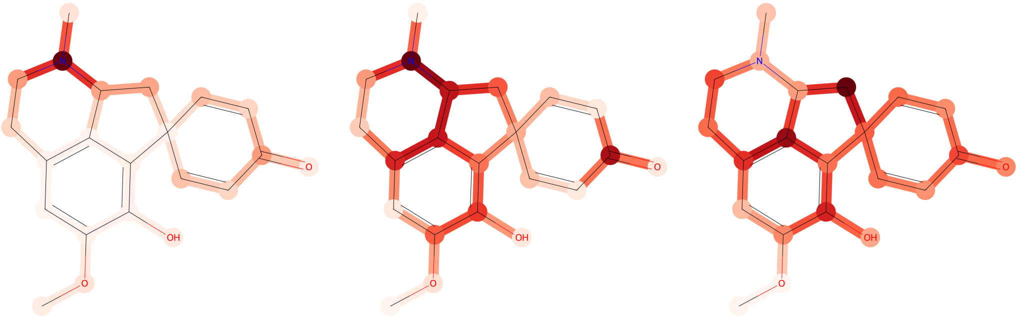

(d) LogP (e) 2-4 (f) five

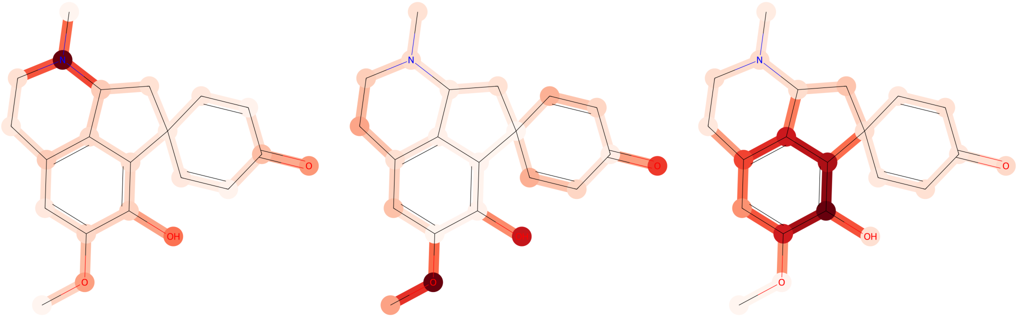

(g) hydrogen bond donors (h) acceptors (i) three rules

Figure 13: Visualization of attention for BBBP on molecule COc1cc2CCN(C)C3CC4(C=CC(=O)C=C4)c(c1O)c23

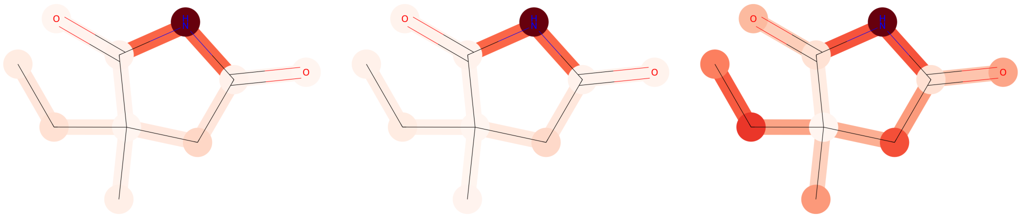

(a) brain blood barrier (b) molecular weight (c) 500

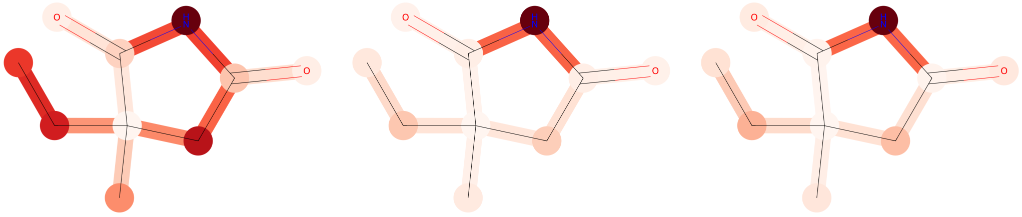

(d) LogP (e) 2-4 (f) five

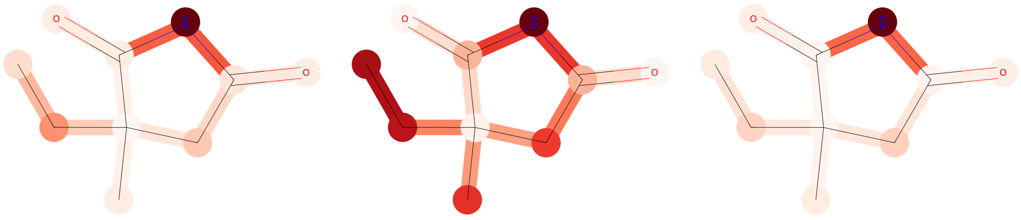

(g) hydrogen bond donors (h) acceptors (i) three rules

Figure 14: Visualization of attention for BBBP on molecule CCC1(C)CC(=O)NC1=O

References

[1] Alayrac, J.-B., Donahue, J., Luc, P., Miech, A., Barr, I., Hasson, Y., Lenc, K., Mensch, A., Millican, K., Reynolds, M., et al. (2022). Flamingo: a visual language model for few-shot learning. *Advances in Neural Information Processing Systems*, 35:23716–23736.

[2] Bachlechner, T., Majumder, B. P., Mao, H., Cottrell, G., and McAuley, J. (2021). Rezero is all you need: Fast convergence at large depth. In *Uncertainty in Artificial Intelligence*, pages 1352–1361. PMLR.

[3] Bagal, V., Aggarwal, R., Vinod, P., and Priyakumar, U. D. (2021). Molgpt: molecular generation using a transformer-decoder model. *Journal of Chemical Information and Modeling*, 62(9):2064–2076.

[4] Bao, H., Dong, L., Piao, S., and Wei, F. (2021). Beit: Bert pre-training of image transformers. *arXiv preprint arXiv:2106.08254*.

[5] Bastos, A., Nadgeri, A., Singh, K., Kanezashi, H., Suzumura, T., and Mulang, I. O. (2022). Investigating expressiveness of transformer in spectral domain for graphs. *arXiv preprint arXiv:2201.09332*.

[6] Brown, T., Mann, B., Ryder, N., Subbiah, M., Kaplan, J. D., Dhariwal, P., Neelakantan, A., Shyam, P., Sastry, G., Askell, A., et al. (2020). Language models are few-shot learners. *Advances in neural information processing systems*, 33:1877–1901.

[7] Casasnovas, R., Ortega-Castro, J., Frau, J., Donoso, J., and Munoz, F. (2014). Theoretical pka calculations with continuum model solvents, alternative protocols to thermodynamic cycles. *International Journal of Quantum Chemistry*, 114(20):1350–1363.

[8] Chen, D., O'Bray, L., and Borgwardt, K. (2022a). Structure-aware transformer for graph representation learning. In *International Conference on Machine Learning*, pages 3469–3489. PMLR.

[9] Chen, X., Wang, X., Changpinyo, S., Piergiovanni, A., Padlewski, P., Salz, D., Goodman, S., Grycner, A., Mustafa, B., Beyer, L., et al. (2022b). Pali: A jointly-scaled multilingual language-image model. *arXiv preprint arXiv:2209.06794*.

[10] Chithrananda, S., Grand, G., and Ramsundar, B. (2020). Chemberta: Large-scale self-supervised pretraining for molecular property prediction. *arXiv preprint arXiv:2010.09885*.

[11] Choromanski, K., Lin, H., Chen, H., Zhang, T., Sehanobish, A., Likhosherstov, V., Parker-Holder, J., Sarlos, T., Weller, A., and Weingarten, T. (2022). From block-toeplitz matrices to differential equations on graphs: towards a general theory for scalable masked transformers. In *International Conference on Machine Learning*, pages 3962–3983. PMLR.

[12] Chung, H. W., Hou, L., Longpre, S., Zoph, B., Tay, Y., Fedus, W., Li, E., Wang, X., Dehghani, M., Brahma, S., et al. (2022). Scaling instruction-finetuned language models. *arXiv preprint arXiv:2210.11416*.

[13] Devlin, J., Chang, M.-W., Lee, K., and Toutanova, K. (2019). Bert: Pre-training of deep bidirectional transformers for language understanding. In *Proceedings of the 2019 Conference of the North American Chapter of the Association for Computational Linguistics: Human Language Technologies, Volume 1 (Long and Short Papers)*, pages 4171–4186.

[14] Dwivedi, V. P. and Bresson, X. (2020). A generalization of transformer networks to graphs. *arXiv preprint arXiv:2012.09699*.

[15] Edwards, C., Lai, T., Ros, K., Honke, G., and Ji, H. (2022). Translation between molecules and natural language. *arXiv preprint arXiv:2204.11817*.

[16] Edwards, C., Zhai, C., and Ji, H. (2021). Text2mol: Cross-modal molecule retrieval with natural language queries. In *Proceedings of the 2021 Conference on Empirical Methods in Natural Language Processing*, pages 595–607.

[17] Efrat, A. and Levy, O. (2020). The turking test: Can language models understand instructions? *arXiv preprint arXiv:2010.11982*.

[18] Fang, Y., Zhang, Q., Yang, H., Zhuang, X., Deng, S., Zhang, W., Qin, M., Chen, Z., Fan, X., and Chen, H. (2022). Molecular contrastive learning with chemical element knowledge graph. In *Proceedings of the AAAI Conference on Artificial Intelligence*, volume 36, pages 3968–3976.

[19] Gaulton, A., Bellis, L. J., Bento, A. P., Chambers, J., Davies, M., Hersey, A., Light, Y., McGlinchey, S., Michalovich, D., Al-Lazikani, B., et al. (2012). Chembl: a large-scale bioactivity database for drug discovery. *Nucleic acids research*, 40(D1):D1100–D1107.

[20] Gilmer, J., Schoenholz, S. S., Riley, P. F., Vinyals, O., and Dahl, G. E. (2017). Neural message passing for quantum chemistry. In *International conference on machine learning*, pages 1263–1272. PMLR.

[21] Gosselet, F., Loiola, R. A., Roig, A., Rosell, A., and Culot, M. (2021). Central nervous system delivery of molecules across the blood-brain barrier. *Neurochemistry International*, 144:104952.

[22] Guo, L., Zhang, Q., and Chen, H. (2022). Unleashing the power of transformer for graphs. *arXiv preprint arXiv:2202.10581*.

[23] Hassani, K. and Khasahmadi, A. H. (2020). Contrastive multi-view representation learning on graphs. In *International conference on machine learning*, pages 4116–4126. PMLR.

[24] Honda, S., Shi, S., and Ueda, H. R. (2019). Smiles transformer: Pre-trained molecular fingerprint for low data drug discovery. *arXiv preprint arXiv:1911.04738*.

[25] Hu, W., Liu, B., Gomes, J., Zitnik, M., Liang, P., Pande, V., and Leskovec, J. (2019). Strategies for pre-training graph neural networks. *arXiv preprint arXiv:1905.12265*.

[26] Kim, J., Nguyen, T. D., Min, S., Cho, S., Lee, M., Lee, H., and Hong, S. (2022). Pure transformers are powerful graph learners. *arXiv preprint arXiv:2207.02505*.

[27] Kreuzer, D., Beaini, D., Hamilton, W., Létourneau, V., and Tossou, P. (2021). Rethinking graph transformers with spectral attention. *Advances in Neural Information Processing Systems*, 34:21618–21629.

[28] Li, J., Li, D., Savarese, S., and Hoi, S. (2023). Blip-2: Bootstrapping language-image pre-training with frozen image encoders and large language models. *arXiv preprint arXiv:2301.12597*.

[29] Liu, L., Liu, X., Gao, J., Chen, W., and Han, J. (2020). Understanding the difficulty of training transformers. In *2020 Conference on Empirical Methods in Natural Language Processing, EMNLP 2020*, pages 5747–5763. Association for Computational Linguistics (ACL).

[30] Liu, S., Demirel, M. F., and Liang, Y. (2019a). N-gram graph: Simple unsupervised representation for graphs, with applications to molecules. *Advances in neural information processing systems*, 32.

[31] Liu, S., Nie, W., Wang, C., Lu, J., Qiao, Z., Liu, L., Tang, J., Xiao, C., and Anandkumar, A. (2022). Multi-modal molecule structure-text model for text-based retrieval and editing. *arXiv preprint arXiv:2212.10789*.

[32] Liu, S., Wang, H., Liu, W., Lasenby, J., Guo, H., and Tang, J. (2021). Pre-training molecular graph representation with 3d geometry. In *International Conference on Learning Representations*.

[33] Liu, Y., Ott, M., Goyal, N., Du, J., Joshi, M., Chen, D., Levy, O., Lewis, M., Zettlemoyer, L., and Stoyanov, V. (2019b). Roberta: A robustly optimized bert pretraining approach. *arXiv preprint arXiv:1907.11692*.

[34] Maziarka, Ł., Danel, T., Mucha, S., Rataj, K., Tabor, J., and Jastrzkebski, S. (2020). Molecule attention transformer. *arXiv preprint arXiv:2002.08264*.

[35] Mialon, G., Chen, D., Selosse, M., and Mairal, J. (2021). Graphit: Encoding graph structure in transformers. *arXiv preprint arXiv:2106.05667*.

[36] Mishra, S., Khashabi, D., Baral, C., Choi, Y., and Hajishirzi, H. (2021). Reframing instructional prompts to gptk's language. *arXiv preprint arXiv:2109.07830*.

[37] Mishra, S., Khashabi, D., Baral, C., and Hajishirzi, H. (2022). Cross-task generalization via natural language crowdsourcing instructions. In *Proceedings of the 60th Annual Meeting of the Association for Computational Linguistics (Volume 1: Long Papers)*, pages 3470–3487.

[38] Nielsen, M. H., Pedersen, F. S., and Kjems, J. (2005). Molecular strategies to inhibit hiv-1 replication. *Retrovirology*, 2:1–20.

[39] Ouyang, L., Wu, J., Jiang, X., Almeida, D., Wainwright, C., Mishkin, P., Zhang, C., Agarwal, S., Slama, K., Ray, A., et al. (2022). Training language models to follow instructions with human feedback. *Advances in Neural Information Processing Systems*, 35:27730–27744.

[40] Park, W., Chang, W.-G., Lee, D., Kim, J., et al. (2022). Grpe: Relative positional encoding for graph transformer. In *ICLR2022 Machine Learning for Drug Discovery*.

[41] Parmar, M., Mishra, S., Purohit, M., Luo, M., Mohammad, M., and Baral, C. (2022). In-boxbart: Get instructions into biomedical multi-task learning. In *Findings of the Association for Computational Linguistics: NAACL 2022*, pages 112–128.

[42] Raffel, C., Shazeer, N., Roberts, A., Lee, K., Narang, S., Matena, M., Zhou, Y., Li, W., and Liu, P. J. (2020). Exploring the limits of transfer learning with a unified text-to-text transformer. *The Journal of Machine Learning Research*, 21(1):5485–5551.

[43] Ramsundar, B., Eastman, P., Walters, P., and Pande, V. (2019). *Deep learning for the life sciences: applying deep learning to genomics, microscopy, drug discovery, and more*. O'Reilly Media.

[44] Rong, Y., Bian, Y., Xu, T., Xie, W., Wei, Y., Huang, W., and Huang, J. (2020). Self-supervised graph transformer on large-scale molecular data. *Advances in Neural Information Processing Systems*, 33:12559–12571.

[45] Ross, J., Belgodere, B., Chenthamarakshan, V., Padhi, I., Mroueh, Y., and Das, P. (2022). Molformer: Large scale chemical language representations capture molecular structure and properties.

[46] Sanh, V., Webson, A., Raffel, C., Bach, S. H., Sutawika, L., Alyafeai, Z., Chaffin, A., Stiegler, A., Scao, T. L., Raja, A., et al. (2021). Multitask prompted training enables zero-shot task generalization. *arXiv preprint arXiv:2110.08207*.

[47] Schick, T. and Schütze, H. (2021). Exploiting cloze-questions for few-shot text classification and natural language inference. In *Proceedings of the 16th Conference of the European Chapter of the Association for Computational Linguistics: Main Volume*, pages 255–269.

[48] Seidl, P., Vall, A., Hochreiter, S., and Klambauer, G. (2023). Enhancing activity prediction models in drug discovery with the ability to understand human language. *arXiv preprint arXiv:2303.03363*.

[49] Su, B., Du, D., Yang, Z., Zhou, Y., Li, J., Rao, A., Sun, H., Lu, Z., and Wen, J.-R. (2022). A molecular multimodal foundation model associating molecule graphs with natural language. *arXiv preprint arXiv:2209.05481*.

[50] Sun, F.-Y., Hoffman, J., Verma, V., and Tang, J. (2020). Infograph: Unsupervised and semi-supervised graph-level representation learning via mutual information maximization. In *International Conference on Learning Representations*.

[51] Sun, M., Xing, J., Wang, H., Chen, B., and Zhou, J. (2021). Mocl: Data-driven molecular fingerprint via knowledge-aware contrastive learning from molecular graph. In *Proceedings of the 27th ACM SIGKDD Conference on Knowledge Discovery & Data Mining*, pages 3585–3594.

[52] Sun, R., Dai, H., and Yu, A. W. (2022). Does gnn pretraining help molecular representation? *Advances in Neural Information Processing Systems*, 35:12096–12109.

[53] Suresh, S., Li, P., Hao, C., and Neville, J. (2021). Adversarial graph augmentation to improve graph contrastive learning. *Advances in Neural Information Processing Systems*, 34:15920–15933.

[54] Taylor, R., Kardas, M., Cucurull, G., Scialom, T., Hartshorn, A., Saravia, E., Poulton, A., Kerkez, V., and Stojnic, R. (2022). Galactica: A large language model for science. *arXiv preprint arXiv:2211.09085*.

[55] Vaswani, A., Shazeer, N., Parmar, N., Uszkoreit, J., Jones, L., Gomez, A. N., Kaiser, Ł., and Polosukhin, I. (2017). Attention is all you need. *Advances in neural information processing systems*, 30.

[56] Velickovic, P., Fedus, W., Hamilton, W. L., Liò, P., Bengio, Y., and Hjelm, R. D. (2019). Deep graph infomax. *ICLR (Poster)*, 2(3):4.

[57] Wang, S., Guo, Y., Wang, Y., Sun, H., and Huang, J. (2019). Smiles-bert: large scale unsupervised pre-training for molecular property prediction. In *Proceedings of the 10th ACM international conference on bioinformatics, computational biology and health informatics*, pages 429–436.

[58] Wang, Y., Magar, R., Liang, C., and Barati Farimani, A. (2022a). Improving molecular contrastive learning via faulty negative mitigation and decomposed fragment contrast. *Journal of Chemical Information and Modeling*, 62(11):2713–2725.

[59] Wang, Y., Min, Y., Shao, E., and Wu, J. (2021). Molecular graph contrastive learning with parameterized explainable augmentations. In *2021 IEEE International Conference on Bioinformatics and Biomedicine (BIBM)*, pages 1558–1563. IEEE.

[60] Wang, Y., Mishra, S., Alipoormolabashi, P., Kordi, Y., Mirzaei, A., Naik, A., Ashok, A., Dhanasekaran, A. S., Arunkumar, A., Stap, D., et al. (2022b). Super-naturalinstructions: Generalization via declarative instructions on 1600+ nlp tasks. In *Proceedings of the 2022 Conference on Empirical Methods in Natural Language Processing*, pages 5085–5109.

[61] Withnall, M., Chen, H., and Tetko, I. V. (2018). Matched molecular pair analysis on large melting point datasets: a big data perspective. *ChemMedChem*, 13(6):599–606.

[62] Wu, Z., Jain, P., Wright, M., Mirhoseini, A., Gonzalez, J. E., and Stoica, I. (2021). Representing long-range context for graph neural networks with global attention. *Advances in Neural Information Processing Systems*, 34:13266–13279.

[63] Xia, J., Wu, L., Chen, J., Hu, B., and Li, S. Z. (2022). Simgrace: A simple framework for graph contrastive learning without data augmentation. In *Proceedings of the ACM Web Conference 2022*, pages 1070–1079.

[64] Xu, D., Cheng, W., Luo, D., Chen, H., and Zhang, X. (2021). Infogcl: Information-aware graph contrastive learning. *Advances in Neural Information Processing Systems*, 34:30414–30425.

[65] Ying, C., Cai, T., Luo, S., Zheng, S., Ke, G., He, D., Shen, Y., and Liu, T.-Y. (2021). Do transformers really perform badly for graph representation? *Advances in Neural Information Processing Systems*, 34:28877–28888.

[66] You, Y., Chen, T., Shen, Y., and Wang, Z. (2021). Graph contrastive learning automated. In *International Conference on Machine Learning*, pages 12121–12132. PMLR.

[67] You, Y., Chen, T., Sui, Y., Chen, T., Wang, Z., and Shen, Y. (2020). Graph contrastive learning with augmentations. *Advances in neural information processing systems*, 33:5812–5823.

[68] Zeng, Z., Yao, Y., Liu, Z., and Sun, M. (2022). A deep-learning system bridging molecule structure and biomedical text with comprehension comparable to human professionals. *Nature communications*, 13(1):862.

[69] Zhang, J., Zhang, H., Xia, C., and Sun, L. (2020). Graph-bert: Only attention is needed for learning graph representations. *arXiv preprint arXiv:2001.05140*.

[70] Zhang, Z., Liu, Q., Wang, H., Lu, C., and Lee, C.-K. (2021). Motif-based graph self-supervised learning for molecular property prediction. *Advances in Neural Information Processing Systems*, 34:15870–15882.

[71] Zhao, H., Ma, S., Zhang, D., Deng, Z.-H., and Wei, F. (2022). Are more layers beneficial to graph transformers? In *The Eleventh International Conference on Learning Representations*.

[72] Zhong, R., Lee, K., Zhang, Z., and Klein, D. (2021). Adapting language models for zero-shot learning by meta-tuning on dataset and prompt collections. In *Findings of the Association for Computational Linguistics: EMNLP 2021*, pages 2856–2878.